MODELING THE STATIC-DYNAMIC FRACTURE IN REINFORCED CONCRETE

Luis Saucedo[1], Rena C. Yu[2] and Gonzalo Ruiz[3]

Departamento de Mecánica Aplicada e Ingeniería de Proyectos,
E.T.S. de Ingenieros de Caminos, Canales y Puertos,
Universidad de Castilla-La Mancha, Avda Camilo José Cela s/n, 13005 Ciudad Real, España

[1]E-mail: luis_saucedo@hotmail.es
[2]E-mail: rena@uclm.es
[3]E-mail: Gonzalo.Ruiz@uclm.es

ABSTRACT

We aim to model the static-dynamic fracture, often propagates in mixed-mode in lightly reinforced concrete beams. When a beam does not have enough shear reinforcement, fracture can initiate and propagate unstably and lead to failure through diagonal tension. In order to study this phenomenon numerically, a model capable of dealing with both static and dynamic crack propagation as well as the natural transition of these two regimes is necessary. A cohesive model for concrete fracture and an interface model for the deterioration between concrete and steel re-bar, both combined with an insertion algorithm, are chosen for this task. The static process is solved by dynamic relaxation (DR) method together with a modified technique to enhance the convergence rate. This same DR method is used to detect a dynamic process and switch to a dynamic calculation. The numerically obtained load-displacement curves, load-CMOD curves and crack patterns fit very well with their experimental counterparts, having in mind that we fed the calculations only with parameters measured experimentally.

KEY WORDS: Diagonal-tension failure, Dynamic relaxation.

1. INTRODUCTION

In this paper we investigate the evolution of 3D mixed-mode fracture in notched reinforced concrete beams subjected to static loading. As observed in the experimental results of Carmona, Ruiz & Del Viso 2007, under static loading conditions, mix-mode fracture can propagate in static or dynamic regime. The conditions of transition between these two regimes vary with beam geometry, reinforcement ratio, location and inclination of the rebar. Knowing those conditions beforehand is essential to beam design and safety of a whole structure, since without a rebar to slow down and eventually stop the dynamic fracture, the beam would collapse. The idea of adding reinforcements to transform a brittle behavior --beam collapsing-- into a ductile one --rebar yielding-- is many times more important than sole increasing of peak loads. In other words, mere high peak load may present false high load capacity if ductility is lacking.

When a beam is not sufficiently reinforced to resist shear, the crack initiated from the notch can run unstably and leads to diagonal tension failure, see Figure 1. To numerically reproduce this entire progress of the crack initiation, propagation and "hinge" forming, is undoubtedly a challenging task. A computational model that is able to not only handle both static and dynamic fracture but also detect the transition in between is required. To tackle this problem, we adopt an explicit discrete cohesive model, with a three-dimensional discretization, incorporated with a modified dynamic relaxation (DR) method. The modified DR, see Yu and Ruiz, 2004, is served both as a solver and a detector for dynamic processes.

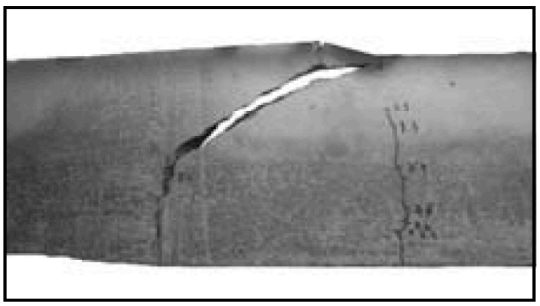

Figure 1. A lightly reinforced concrete beam failed through diagonal tension.

2. FINITE ELEMENT METHODOLOGY

We model the concrete bulk using the Neo-Hookean material extended to the compressible range. The fracture in concrete is modeled using a 3D cohesive model developed by Ortiz & Pandolfi 1999, with a linear-decreasing cohesive law. The steel rebar is explicitly represented using 10-node tetrahedrons and follows an elastic perfectly-plastic constitutive law. The steel-concrete interface is simulated through an interface

element endorsed with a perfectly plastic bond-slip law. Both the cohesive elements and the interface elements are inserted upon crack initiation or bond deterioration, the geometry is updated through an effective fragmentation algorithm, see Pandolfi & Ortiz, 2002. The whole process is solved using a modified dynamic relaxation method (Yu & Ruiz 2004). All the material properties were measured through independent experiments and their values are listed in Table 1, where E represents the material elastic modulus, f_t ,G_F are the tensile strength and the specific fracture energy of the concrete, $S_{c0.2}$ stands for the 0.2% yield strength of the steel rebar, T_c is the bond strength of the steel-concrete interface. Note that the value 174 GPa is the nominal modulus measured for a ribbed rebar.

Table 1. Mechanical properties of concrete, steel and the interface in between given in Carmona, Ruiz & Del Viso 2007.

Material	E (GPa)	f_t (MPa)	G_F (N/m)	$S_{c0.2}$ (MPa)	T_c (MPa)
Concrete	*36.3*	*3.8*	*43.4*	-	-
Steel	*174*	-	-	*563*	-
Steel-Concrete interface	-	-	-	-	*6.4*

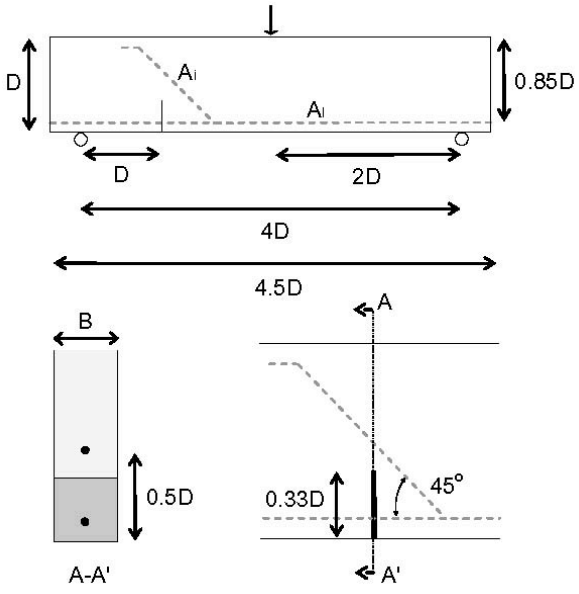

Figure 2. Geometry for the beams tested by Carmona, Ruiz & Del Viso (2007), where D is of 75, 150 and 300 mm for small (S), middle (M) and large (L) specimens.

3. NUMERICAL RESULTS

3.1. Validation

In Figure 2, we show the geometry of the notched beams tested by Carmona, Ruiz and Del Viso (2007) and follow their nomenclature for a beam of different size (S, M or L), reinforced with longitudinal or shear steel bars. For example, S01 is a small size beam, with zero longitudinal, one transversal rebar. This was designed to provoke a single propagating crack in beams of different sizes and to facilitate the study of crack trajectories, peak loads and their relation with the amount and location of the reinforcements.

Beams M00 and M20 are chosen as validation examples. The complete load-displacement and load-CMOD curves are plotted against their experimental counterparts in Figure 3, where letters A to E mark different stages of the crack propagation. Taking into consideration that all fed material parameters are measured ones, the fit is remarkable.

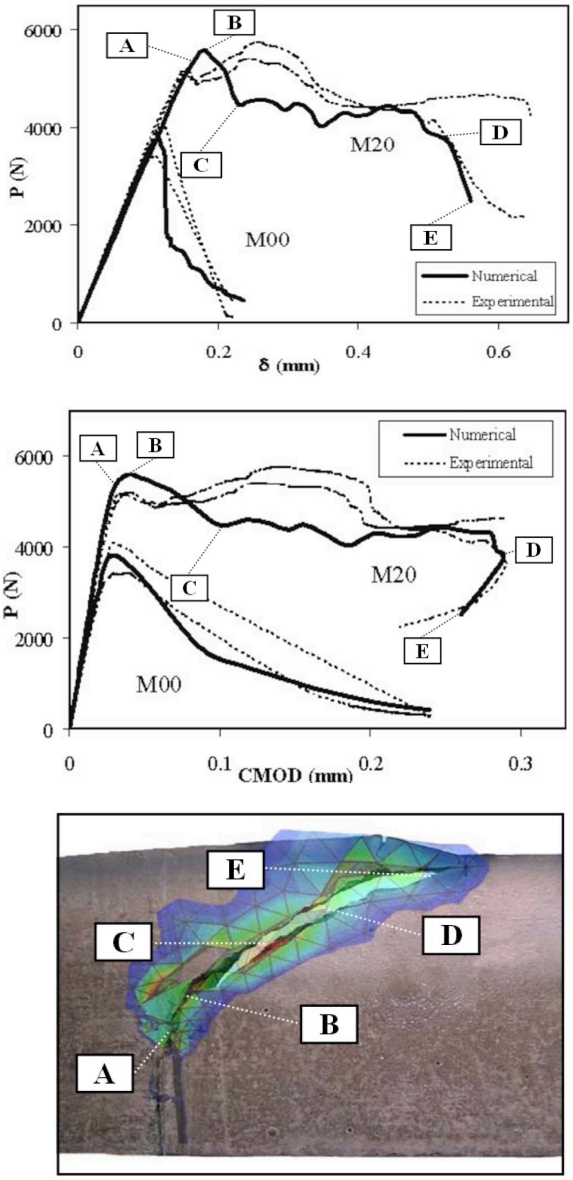

Figure 3. Numerical-experimental comparison for (from top to bottom) load-displacement, load-CMOD curves and crack patterns.

It needs to be pointed out that, the calculations shown in Figure 3 had gone through a static-dynamic-static transition. In particular, at the last stage of M20, the crack closes due to the formation of the "hinge" after the diagonal-tension failure. This last part cannot be captured by any sophisticated solvers if considering it static, since the crack propagation is intrinsically dynamic. The lower numerical load at post-peak compared to the experimental one is attributed to the material hardening of the rebar is not yet included in the numerical model.

3.2. Dynamic fracture under static loading

When a structural element fails due to surpassing of its loading limit, the collapsing process is usually unstable, and is accompanied with dynamic fracture. Such a dynamic fracture propagation under static loading is demonstrated in Figure 4 for the case of a small beam without any reinforcements S00. Figure 4(top) shows the numerical crack trajectory superimposed upon the experimental one. A perfect match is obtained. In Figure 4(bottom), the discontinuous lines with empty symbols represent the experimentally recorded load-displacement curve. Note that, at post-peak stage, from peak load to zero load, no intermediate points were recorded due to the rapid failure of the beam. In other words, we cannot directly compare the load-displacement data after peak load, nevertheless, one can observe that the numerical softening curve tends to the experimental one taken at the end of the experiment. The matching of both the load-displacement curves and crack trajectories validates both the amount and the location of the energy spent. It needs to be pointed out that since the test was done with displacement control, it was the self-weight that provoked the dynamic fracture when the crack was advanced towards the loading plane. For a beam with reinforcements, the static-dynamic transition could occur (a) when the interface is broken and (b) when the rebar is yielded or broken, see Figure 3 B-C and D-E, and Figure 4 B-C. Figure 3 shows that the longitudinal reinforcement of M20 actually stopped the dynamic crack propagation, consequently there was a dynamic-static transition from point C to D, apart from the static-dynamic ones B-C and D-E. Such transitions are determined by the reinforcement ratio and the beam geometry.

3.3. Effect of longitudinal and transversal reinforcements

From Figure 3, comparing the case of M00 and M20, we observe that longitudinal rebars help to augment both the peak and the ultimate loads. Consequently, M20 is more ductile compared to the non-reinforced one M00. From Figures 4 and 5, for beam S01, however, the peak load is lower than the beam S00. By looking at the crack trajectories, we observe that the transversal rebar served to change the main crack trajectory at point D. This is clearly seen in Figure 6, where the experimental trajectories are put together for beams S00, S01, S10 and S11. The fractures paths remained the same at the first stage of the crack propagation, this shows neither the longitudinal nor the transversal rebar was activated.

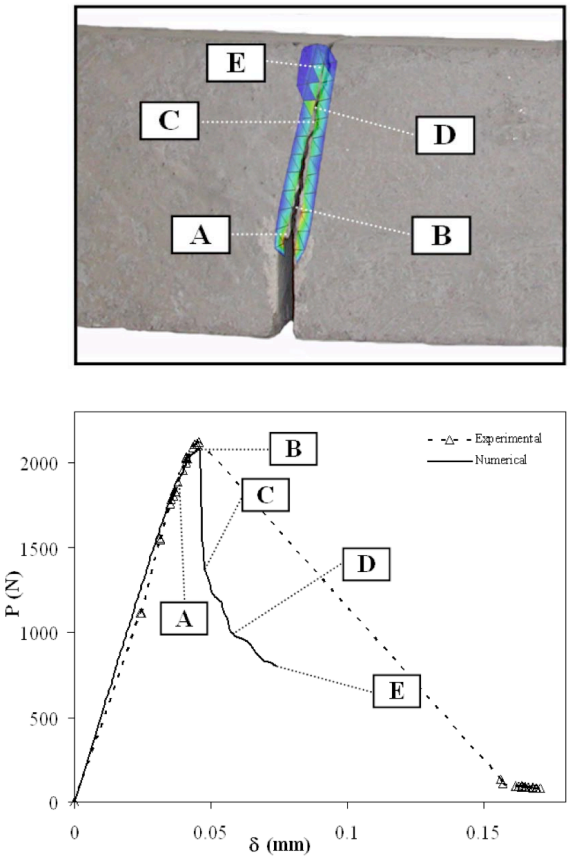

Figure 4. Experimental and numerical comparison for (top) crack patterns and (bottom) load-displacement curve for the case of S00, a small beam with neither longitudinal nor transversal reinforcements.

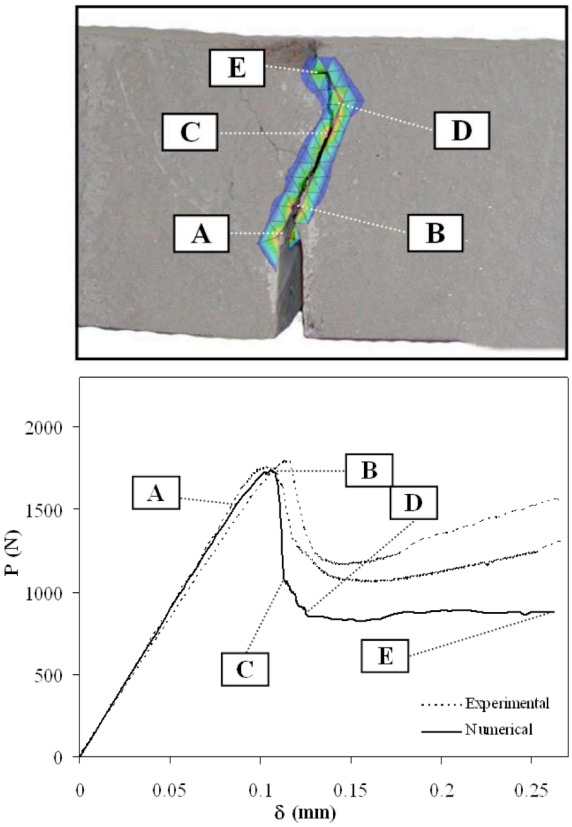

Figure 5. Numerical and experimental crack patterns and load-displacement curve for S01, a small beam reinforced with one transversal re-bar.

Then the crack path curved towards the loading plane for S10, whereas it went the opposite direction for S01. The crack followed a straight line in the case of S00. S11 is a mixture of S01 and S10, but closer to S10 than to S01. This reveals the stronger influence of the longitudinal reinforcement than the transversal on fracture path. It bears emphasis that such complicated trajectory would be an impossible task for those methods that work with only pre-embedded cracks.

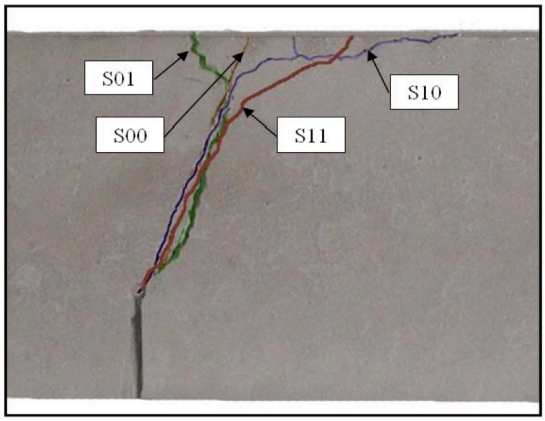

Figure 6.Main crack trajectories observed in experiments for beams S00, S01, S10 and S11.

3.4 Size effect in reinforced beams

According to the size effect law, two geometrically similar beams, the smaller one resists proportionally more than the larger one. However, Figure 7 shows the well-distinguished smaller-is-stronger rule in plain concrete beams do not equally reproduce for reinforced ones. In Figure 7(top), the load-displacement values for S10 are doubled to compare better with M20. Surprisingly, S10 resists less peak load than M20.

By looking at the movements of the two crack surfaces individually, see Figure 7(bottom), we observe that S10 and M20 show different failure mechanisms. Larger absolute amount of reinforcement in M20 has resulted that the left part of the beam is being dragged towards the loading plane. In other words, even though S10 and M20 share the same crack patterns, but the loading capacity do no follow the size effect law as observed in plain concrete beams. This phenomenon would not be captured by a non-explicit representation of the rebar and cracks.

3.5. Dowel action and sewing effect of the rebar

Figure 8 is a snapshot of the fractured beam S11, reinforced with one longitudinal and one transversal rebar. Note that the phenomenon of dowel action as shear transfer mechanism across cracks is reproduced naturally as a result of the explicit representation of rebar and the bond-slip interaction between concrete bulk and the rebar. Additionally observed is the sewing effect of both rebars and secondary cracks in concrete bulk. Correctly model each physical phenomenon individually and the interactions between reinforcement and concrete is fundamental for a right design of an reinforced concrete structure, since all those aforementioned factors contribute to the entire energy consumption therefore the resistance and global behavior of the beam.

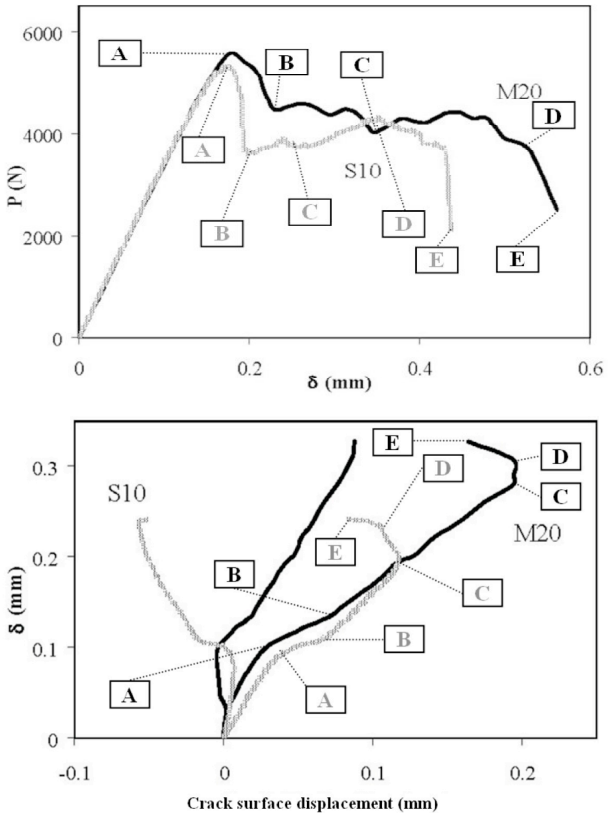

Figure 7. Load-displacement comparison for S10 and M20 (top) and crack surface displacements versus loading-point displacement for S10 and M20 (bottom).

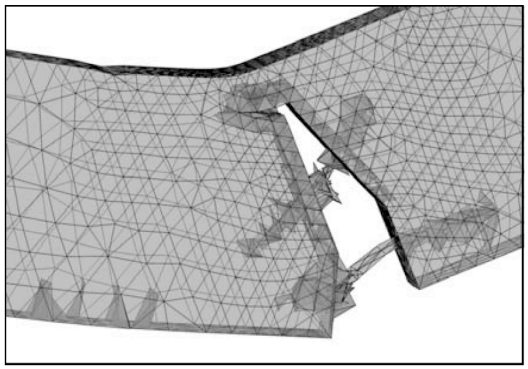

Figure 8. The dowel action, sewing effect of the rebar and secondary cracks modeled in beam S11.

4. CONCLUSIONS

We have modeled the static-dynamic mixed-mode fracture in reinforced concrete. The concrete bulk, steel rebar and the interface in between are all explicitly represented. A modified relaxation method is employed to solve the static process and detect a dynamic one. The methodology was validated against experimental results of Carmona, Ruiz and Del Viso. The salient features, such as micro cracking, changing of crack trajectory, pull out and the dowel action of the rebar, are all naturally reproduced through the discrete fracture and explicit representation of the rebar. As a by-product, the fundamental role of fracture mechanics in reinforced concrete structure design is thoroughly demonstrated.

ACKNOWLEDGEMENTS

The authors acknowledge the financial support from *Ministerio de Ciencia e Innovación,* Spain, under grant MAT 2006-09105 and the Consejería de Educación y Ciencia, JCCM, Spain, under grant PAI08-0196.

REFERENCES

Yu, R.C. and Ruiz, G. 2004 Multi-cracking modeling in concrete solved by a modified DR method. *Computers and Concrete*, **1(4)**, 371-388.

Carmona, J.R., Ruiz, G. and Del Viso, J.R. Mixed-mode crack propagation through reinforced concrete. Engineering Fracture Mechanics. *Engineering Fracture Mechanics,* **74**, 2788-2809.

Ortiz, M. and Pandolfi, A. 1999 Finite-deformation irreversible cohesive elements for three-dimensional crack-propagation analysis. *International Journal for Numerical Methods in Engineering*, **44**:1267-1282.

Pandolfi, A. and Ortiz, M. 2002 An efficient adaptive procedure for three-dimensional fragmentation simulations. *Engineering with Computers*, **18**:148-159.